

Debye-Waller factor in solid ^4He crystals

C. A. Burns

Department of Physics, Western Michigan University, Kalamazoo, Michigan 49008

E. D. Isaacs

Bell Laboratories, Lucent Technologies, 600 Mountain Avenue, Murray Hill, New Jersey 07974

(Received 7 October 1996)

We report synchrotron x-ray-diffraction measurements on low-density hcp-solid ^4He at a temperature of ~ 0.7 K. The root-mean-square deviation of the atoms from their lattice positions $\langle u^2 \rangle^{1/2}$ is determined from measurements of the Debye-Waller factor at the (002), (004), and (006) Bragg peaks. We find $\langle u^2 \rangle^{1/2} = 0.96 \pm 0.02$ Å along the c axis. Our results are consistent with Green's function-Monte Carlo calculations. Weak reflections at the hcp-forbidden (001) and (003) Bragg peaks were also observed, probably indicating structural defects in the crystals. [S0163-1829(97)00610-3]

I. INTRODUCTION

Quantum crystals are interesting because of the large amplitude zero-point oscillations of the basis atoms about their lattice sites. This amplitude is a large fraction of the interatomic spacing, and so theoretical models of these solids must deal with the strong hard-core repulsion between the atoms, as well as the large anharmonic terms in the potential. Due to their low mass and the weak interatomic attraction, solid ^3He and ^4He exhibit these effects most strongly. Scattering experiments are especially valuable probes of these crystals, since they can be directly related to microscopic properties, and therefore offer quantitative tests of microscopic models.

The purpose of these measurements was to show that synchrotron x-ray diffraction can be used to measure the zero-point motion of the atoms. By measuring the Debye-Waller factor as a function of reciprocal-lattice vector we were able to determine the amplitude of the zero-point oscillations in low-density solid ^4He . We found that the atoms were undergoing oscillations with a rms value of 0.96 ± 0.02 Å along the c axis, a value in good agreement with theoretical models of the solid.

II. BACKGROUND

A. General properties

At zero temperature ^4He solidifies at a pressure of 25 atm in an hcp structure. There is a small minimum in the melting curve at a temperature of 0.775 K. A bcc phase exists over a narrow range of temperatures ($1.46 < T < 1.77$ K) and pressures close to the melting pressure. A more detailed description is given by Keller.¹ A general review of the properties of quantum crystals is given by Andreev.²

B. Theories of the ground state

A number of different attempts have been made to calculate the ground-state properties of liquid and solid helium. Early detailed calculations of crystal properties were made

by McMillan using variational wave functions;³ recent improvements in these methods resulted from the use of shadow wave functions.⁴

Despite the improvement in the variational techniques, the most accurate calculations of the ground-state properties of the solid are found using the Green's-function Monte Carlo (GFMC) method. The GFMC method involves numerically integrating the Schrödinger equation for a finite-size system with periodic boundary conditions. These calculations should yield an accurate picture of the system, as long as finite-size effects are corrected for or are insignificant, and the correct potential is used. Calculations for solid helium were carried out by Whitlock *et al.*,⁵ who found a ratio of

$$\frac{\sqrt{\langle u^2 \rangle}}{d} = 0.267 \pm 0.003,$$

where d is the nearest-neighbor distance. No anisotropies along different crystal directions were predicted. These calculations used the Lennard-Jones potential for the interatomic interaction. However, the Lennard-Jones potential may not be a sufficiently accurate model for the true potential,⁶ so a comparison with experiment provides a valuable test of this work.

C. Theories of melting of quantum crystals

A first-principles microscopic theory of the fluid-solid transition for classical systems has been given by Ramakrishnan and Yussouff.⁷ Modifications of this theory for the case of quantum crystals were made by Chui.⁸ In particular, Chui predicts that Lindemann's ratio for quantum solids will be 2.7 times the value found for classical systems, that is the amplitude of vibration near melting should be 27% of the interatomic spacing. In addition, his calculations indicate that the Debye-Waller factors will be greater in the directions that are parallel to the ab planes (by about 12%) than along the c axis. This would imply oscillations of $\sim 24\%$ along the c axis. Other theories also predict that the amplitude of the zero-point motion should be anisotropic,⁹ but no anisotropy has yet been observed.

D. Previous neutron studies

A number of neutron-scattering experiments have been carried out on solid helium; the majority of these have concentrated on ^4He since ^3He has a very large absorption cross section for neutrons. A recent review has been given by Glyde.¹⁰

While some information about the extent of zero-point oscillations has been determined by neutron scattering,¹¹ the method suffers from serious difficulties, as has been discussed by Price.¹² Intensity measurements by Minkiewicz and co-workers¹¹ showed oscillations of the intensity as a function of reciprocal-lattice vector instead of the monotonic decrease expected from the Debye-Waller factor. These oscillations were consistent with multiple-scattering effects.¹³ These effects make it impossible to determine the zero-point motion using neutron scattering.

More recently, neutron-scattering measurements have focused on determining the single-particle dynamics of the atoms using deep inelastic neutron scattering to determine the momentum density $n(\mathbf{p})$ of the individual atoms and thereby deduce the average kinetic energy per atom. A recent review on work in quantum liquids was given by Sokol,¹⁴ and the status in solid helium was reviewed by Simmons.¹⁵ Studies on the hcp phase have been carried out by Hilleke *et al.*,¹⁶ while Sokol and co-workers¹⁷ have examined the bcc phase. These results have generally agreed with theoretical models of the solid.

E. Previous x-ray studies

X-ray studies were first used to determine the crystal structure of solid He.¹⁸ Simultaneous x-ray and sound velocity measurements were made by Greywall¹⁹ in order to determine the orientation dependence of the sound velocity. Extensive work was carried out by Simmons and collaborators, who studied vacancies in pure ^3He and ^4He crystals as well as solid mixtures.²⁰ More recently, inelastic x-ray-scattering measurements have been used to determine the electronic excitations in the solid.²¹ We are unaware of any x-ray measurements of the Debye-Waller factor in the low density solid.

F. X-ray-diffraction methods

The c/a ratio for solid ^4He is 1.63 over a wide range of pressures,²² which is the ratio expected for close-packed spheres. We can therefore treat the solid as an ideal hcp structure. The c -axis parameter for our crystals is 5.985 Å, while the lattice parameter along the a and b directions is 3.67 Å. The absorption length in the solid can be computed using tabulated mass absorption coefficients²³ and is 12.6 cm for our x-ray wavelength of 1.63 Å. Since our crystal is only 1.25 cm in diameter, absorption effects are small. We also believe that crystal quality is insufficient to result in significant extinction effects. Some evidence for this is discussed below.

The measured intensity of an x-ray rocking curve where extinction effects and absorption effects are insignificant is given by the integrated intensity²³ I_i multiplied by the Debye-Waller factor²⁴

$$I = I_i \exp\left[-\frac{1}{3}\langle u^2 \rangle G^2\right], \quad (1)$$

$$I_i = \frac{I_0 e^4 \lambda^3 \delta V}{2 \omega m^2 c^4 \nu_a^2} F_{hkl}^2 \frac{\cos^2 2\theta}{\sin 2\theta}, \quad (2)$$

where $\langle u^2 \rangle$ is the mean-square deviation of the atoms about their lattice sites, and G is the reciprocal-lattice vector. I_0 is the intensity of the beam, e is the electron charge, λ is the x-ray wavelength, δV is the volume of the crystal, ω is the rotation frequency used during the scan, m is the mass of the electron, c is the speed of light, and ν_a is the volume per atom. F_{hkl} is the structure factor for the hkl reflection, and the $\cos^2 2\theta$ term is the polarization factor which arises for our scattering geometry. In writing the polarization term this way we are ignoring a small component out of the plane of the ring; for our measurements the correction due to this term is only a few percent.

It should be noted that the Debye-Waller exponent in general contains higher-order terms in the expansion, such as $\langle u^4 \rangle G^4$. However, our data is well fit by the standard form used in Eq. (1), and our measurements are not sufficient to determine the extent (if any) of higher-order terms in the expansion.

Since the hcp structure has two atoms in the basis we need to consider the structure factors for different reflections. For the hcp structure the relations relevant to our work are

$$\begin{aligned} h + 2k = 3n, \quad l = \text{even}: \quad F_{hkl}^2 &= 4f^2, \\ h + 2k = 3n, \quad l = \text{odd}: \quad F_{hkl}^2 &= 0, \end{aligned} \quad (3)$$

where f is the atomic form factor for helium, which is tabulated.²⁵

In the usual case, the vibrations are due to the thermal energy of the atoms, and Eq. (1) is rewritten in terms of the temperature. However, in our case the vibrations are due to the zero-point energy. By measuring the intensity of the reflections as a function of G and correcting for the dependence of F_{hkl} and the polarization factor at the different G values we can therefore determine $\langle u^2 \rangle^{1/2}$, the extent of the zero-point oscillations.

III. EXPERIMENTAL SETUP

Experimentally, helium is very amenable to investigation. High-purity ^4He (^3He concentration < 1 ppb) is available, and large high-quality crystals are relatively easy to grow. For this work we examined hcp solid ^4He at molar volumes near the maximum molar volume ($\sim 21 \text{ cm}^3$). Molar volume was determined indirectly from the growth temperature using the melting curve data of Grilly.²⁶

Elastic x-ray-scattering measurements were taken on beamline X16B at the National Synchrotron Light Source (NSLS) at Brookhaven National Laboratories. The sample cell was mounted on a platform that was attached to the mixing chamber of an Oxford Instruments Kelvinox dilution refrigerator especially designed for x-ray-scattering research. X-ray access to the low-temperature region is through two vacuum cans and a heat shield all of which have 10 mil thick beryllium windows in order to allow x-ray transmission to the sample cell.

A simplified schematic of the sample cell is shown in Fig. 1. The cell consists of a central region made from a thin (10 mil) cylindrical Be window to allow for x-ray access as well

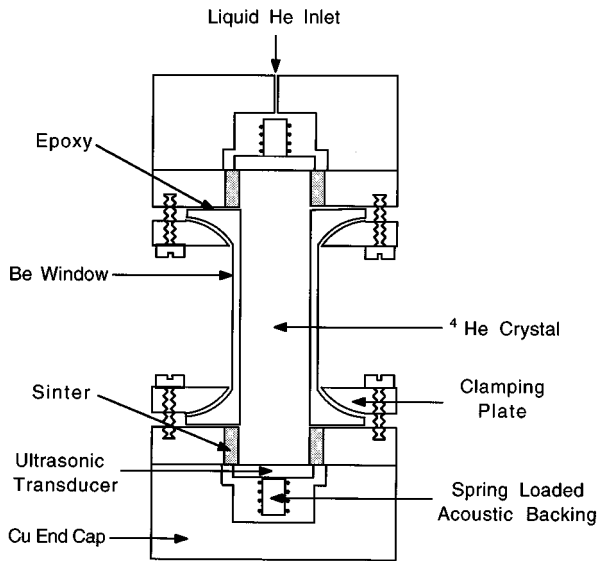


FIG. 1. Simplified schematic of the sample cell. The beryllium window allows x-ray access to the crystal.

as provide a pressure vessel in which to grow the crystal. The Be window thickness was chosen in order to provide sufficient strength to withstand the pressures (~ 25 atm) required to grow the crystals. This window is held against copper endpieces with stainless steel caps. Stycast epoxy 2850 GT is used to make the pressure seal. The copper endpieces were ground flat and parallel after the Be piece was attached in order to align the acoustic transducers. The transducers are held by a spring loaded acoustic backing against the copper pieces. The acoustic transducers were used to optimize crystal growth techniques before carrying out the synchrotron measurements described here. Endcaps are screwed down against indium wire to make a pressure seal at the end of the crystal.

The cell has sintered copper powder in it outside of the x-ray path. The sinter is important for two reasons. First, it provides a good thermal contact between the copper and the helium by increasing the effective surface area of the interface. More importantly, it eliminates rotation of the crystals. Earlier x-ray workers claimed²⁷ that there was a tendency for solid helium crystals to show irreproducible changes due to rotation of the crystals. The part of the crystal that grows in the sinter will be incapable of rotation, and will serve to anchor the rest of the crystal.

Thermally insulating (phenolic) rods attached the top of the sample cell to the mixing chamber of the dilution refrigerator. The top had to be thermally insulating, since attempts to grow the crystals upside down were unsuccessful. The bottom of the cell was put in good thermal contact with the mixing chamber by means of a cold finger consisting of a single copper rod of diameter 0.125", as well as a bundle of Cu wire.

Crystals were grown at constant pressure, since this method has been found to yield large, high-quality single crystals.²⁸ The growth method was as follows. The temperature was set to the desired value, and the pressure was slowly increased until the crystal started to grow as was indicated by shifts in the sound velocity measured by the ultrasonic trans-

ducers. Then the pressure was kept constant (within $\sim 0.02\%$) by manual adjustment of a metering valve until the crystal filled the sample chamber. Afterwards the pressure was slowly increased in order to freeze off the helium in the fill line (and thereby reduce the heat leak through the superfluid in the fill line). The crystal was then cooled to $T \sim 0.7$ K. For the crystal described here we were forced to grow it at a temperature of 1.5 K due to a large heat leak from the superfluid helium in the fill line. The disadvantage of this growth temperature is that the crystal grew in the bcc phase, and underwent a bcc-hcp phase transition upon cooling (as was seen in the x-ray measurements). This transition may have reduced the quality of the crystal.

Measurements were taken in a horizontal scattering geometry. X rays of energy 7.594 keV were selected by an asymmetrically cut singly bent horizontal monochromator [Ge(111)] which focuses two milliradians in the horizontal. The orientation of the crystal was determined using x rays during the run. The structure factor was measured in the liquid during solidification, and then data was taken on the (002), (004), and (006) peaks. In addition, data was taken on the (001) and (003) peaks, which are forbidden [see Eq. (3)] for a perfect crystal. Temperature was determined by measuring the resistivity of a calibrated Lakeshore Germanium resistor. The resistivity was determined using a Linear Research LR-400 bridge with the standard four-wire technique.

IV. DATA AND ANALYSIS

A. Zero-point oscillations

We measured the intensity of several elastic peaks in a solid ^4He crystal grown at a temperature of 1.5 ± 0.1 K. The crystal grew in the bcc phase and underwent a bcc-hcp phase transition upon cooling. The molar volume of the crystal is²⁶ 20.9 cm^3 . Measurements were taken at a temperature $T = 0.7 \pm 0.05$ K. The measured intensities as a function of θ for the (002), (004), and (006) peaks are shown along with the results of Gaussian fits in Fig. 2. The heights of the (002) and the (004) peaks were reduced by factors of 2×10^5 and 2×10^3 , respectively, to allow the qualitative shapes to be compared. The width of the peaks is comparable to the resolution limits of our instrument (about 0.1° for our geometry).

In order to isolate the effects of the zero-point vibration we take the measured intensities, and divide by the structure factor squared as well as the angle-dependent factor. The resulting intensities along with a fit to the data are graphed in Fig. 3. Note that in the absence of atomic vibrations these normalized intensities would be the same. The large reduction in the intensities comes from the Debye-Waller factor due to zero-point motion.

From Eq. (1) it is clear that the slope of the line yields the value for the mean-square deviation. We find a value for the rms deviation about the lattice site of $0.96 \pm 0.02 \text{ \AA}$. These measurements are for planes along the c axis, so we are measuring the atomic deviation along that axis. Thus the atoms vibrate about 16% of the c -axis spacing. Zero-point motion is often expressed as the amplitude of the oscillation as compared to the nearest-neighbor separation. Using the nearest-neighbor separation of 3.67 \AA , we find that the atoms are undergoing a rms deviation of $26.2 \pm 0.6\%$ of the nearest-neighbor distance.

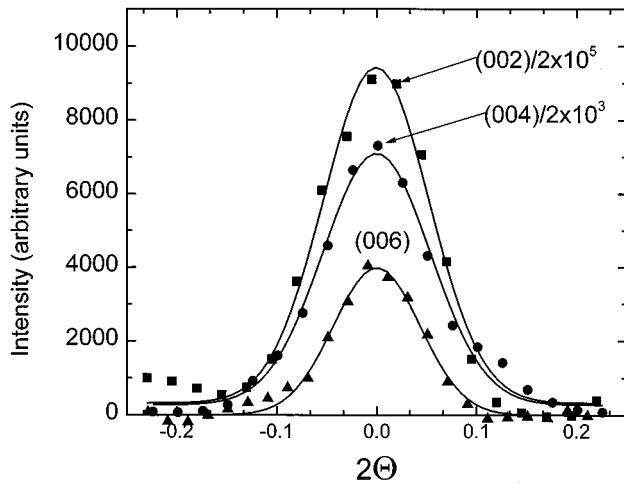


FIG. 2. Raw data from several reflections. A background of about 20% of the maximum intensity has been subtracted from the (006). The intensity of the (002) has been reduced by a factor of 2×10^5 , while the intensity of the (004) has been reduced by 2×10^3 . The solid lines are the results of Gaussian fits to the data.

We wish to compare our results to the GFMC calculations which were made for solid helium at zero temperature, so we need to consider the effect of thermal energies on the atomic vibrations at our measurement temperature of 0.7 K. Kittel²⁹ has shown that for a phonon spectrum described by a Debye model the atomic vibrations are given by

$$K[1 + 2\pi^2/3(T/\Theta_D)^2 + \dots], \quad (4)$$

where K is a constant, the first term in parentheses is the zero-point contribution, and the second term is the first-order correction due to thermal energy. Using Eq. (4) with the measured Debye temperature [$\Theta_D \sim 26$ K (Ref. 30)], we find that the thermal term is less than 0.5% the size of the zero-point term, so the thermal vibrations do not contribute significantly to the measured atomic vibration. Our value of $26.2 \pm 0.6\%$ for the rms deviation agrees quite well with the GFMC method ($26.7 \pm 0.003\%$). Our results therefore show that the theoretical model accurately describes the solid.

When comparing our results with the model of quantum melting, we need to consider the fact that we are measuring the atomic vibrations at a temperature below the melting temperature. Since we are looking at a low melting temperature crystal ($T_m \sim 1.5$ K) the affect of thermal energy on vibrations is small. Using Eq. (4) we see that we would expect an increase in the extent of thermal oscillations of less than 2% for a temperature increase from our measuring temperature (0.7 K) to the melting temperature. Our measured amplitude is different than the result expected from the theory of quantum melting, which is not surprising considering the simplicity of the model. However, the fact that we were only able to look at reflections along the (00 l) direction meant that we were unable to check for the possibility of anisotropic vibrations. A check for anisotropy would be a better test of this aspect of the model.

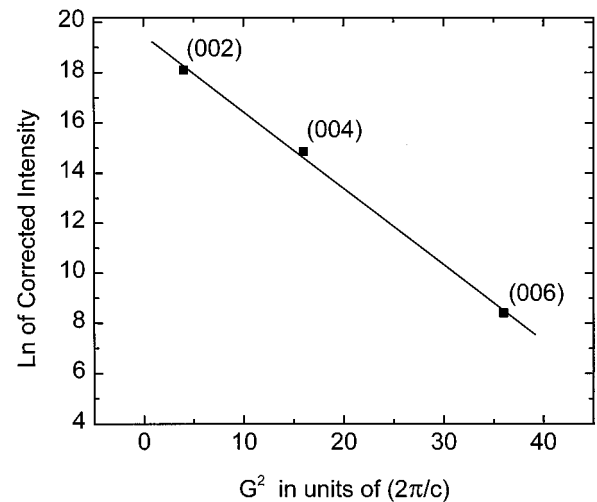


FIG. 3. Graph of corrected intensities vs G^2 (G is in units of $2\pi/c$). In the absence of atomic motion the corrected intensities would all have the same value. The decrease in intensity is due to the Debye-Waller factor arising from quantum zero-point motion. Error bars from the statistical uncertainty are smaller than the data points.

B. Forbidden reflections

We also observed the (001) and (003) reflections. These signals were about a factor of 10^4 weaker than the allowed reflections (when the Debye-Waller factor is corrected for), and there were multiple peaks at the proper 2Θ value. It is unlikely that the forbidden reflections are due to the anharmonic nature of these crystals. Forbidden reflections have been observed in a number of systems such as Si and Ge,³¹ and are due to two separate processes. First, there is a density shift for the electrons due to a lack of inversion symmetry in the crystal—the electrons do not sit exactly on their lattice site. In addition, the anharmonic terms in the potential can also lead to vibrations that favor motion for the electrons in one direction rather than the other, also resulting in weakly allowed forbidden reflections. While anharmonicity in solid helium is thought to make certain forbidden reflections observable,³² these effects are not expected for the (00 l) reflections, since these reflections have inversion symmetry. A more likely explanation is that the reflections are due to strain or a regular stacking fault in the crystal. This strain could have resulted from the bcc-hcp transition in the solid.

V. CONCLUSIONS

We have shown that it is possible to determine the mean-square deviation of the atoms in quantum crystals from x-ray-diffraction measurements of the Debye-Waller factor. Our measurements yield a value of $\langle u^2 \rangle^{1/2} = 0.96 \pm 0.02$ Å, which is in excellent agreement with the value predicted by the GFMC method. This technique promises to be a useful tool for studying these systems. Future work that is of interest is looking for temperature dependence of the atomic motion, looking for crystal anisotropy effects, and making measurements to determine these parameters in solid ^3He .

ACKNOWLEDGMENTS

We would like to acknowledge helpful conversations with Dr. Philip Platzman and Dr. John Goodkind. We would also like to thank Joseph Snyder for his help in fitting data. Fi-

nally, we would like to thank Dr. Dennis Greywall for a critical reading of the manuscript. This work was supported in part by a FRACASF grant from Western Michigan University.

-
- ¹W. E. Keller, *Helium-3 and Helium-4* (Plenum, New York, 1969).
- ²A. F. Andreev, *Progress in Low Temperature Physics* (North Holland, Amsterdam, 1982), Vol. 8, Chap. 2.
- ³W. L. McMillan, *Phys. Rev.* **138**, A442 (1965).
- ⁴T. MacFarland, S. A. Vitiello, L. Reatto, G. V. Chester, and M. H. Kalos, *Phys. Rev. B* **50**, 13 577 (1994).
- ⁵P. A. Whitlock, D. M. Ceperley, G. V. Chester, and M. H. Kalos, *Phys. Rev. B* **19**, 5598 (1979).
- ⁶J. Barker, in *Rare Gas Solids*, edited by M. Klein and J. A. Verables (Academic, New York, 1976).
- ⁷T. V. Ramakrishnan and M. Yussourff, *Phys. Rev. B* **19**, 2775 (1979).
- ⁸S. T. Chui, *Phys. Rev. B* **41**, 796 (1990).
- ⁹D. Rosenwald, *Phys. Rev.* **154**, 160 (1967).
- ¹⁰H. R. Glyde and E. C. Svensson, in *Methods of Experimental Physics* (Academic, New York, 1987).
- ¹¹V. J. Minkiewicz, T. A. Kitchens, G. Shirane, and E. B. Osgood, *Phys. Rev. A* **8**, 1513, (1973); V. J. Minkiewicz, T. A. Kitchens, F. P. Lipsultz, R. Nathans, and G. Shirane, *Phys. Rev.* **174**, 267 (1968).
- ¹²D. L. Price, in *The Physics of Liquid and Solid Helium* (Wiley, New York, 1978).
- ¹³H. R. Glyde, *Can. J. Phys.* **52**, 2281 (1974).
- ¹⁴P. E. Sokol, *Can. J. Phys.* **65**, 1393 (1987).
- ¹⁵R. O. Simmons, *Can. J. Phys.* **65**, 1401 (1987).
- ¹⁶R. O. Hilleke, P. Chaddah, R. O. Simmons, D. L. Price, and S. K. Sinha, *Phys. Rev. Lett.* **52**, 847 (1984).
- ¹⁷P. E. Sokol, R. O. Simmons, D. L. Price, and R. O. Hilleke, in *Proceedings of the 17th International Conference on Low Temperature Physics* (Elsevier, Amsterdam, 1984).
- ¹⁸W. H. Keesom and K. W. Taconis, *Physica* **5**, 161 (1938).
- ¹⁹D. S. Greywall, *Phys. Rev. A* **3**, 2106 (1971).
- ²⁰R. O. Simmons, *J. Phys. Chem. Solids* **55**, 895 (1994), and references within.
- ²¹N. Schell, R. O. Simmons, A. Kaprolat, W. Schülke, and E. Burkel, *Phys. Rev. Lett.* **74**, 2535 (1995).
- ²²J. E. Vos, B. S. Blaise, D. A. Boon, W. J. Van Scherpenzeel, and R. Kingma, *Physica* **37**, 51 (1967).
- ²³B. E. Warren, *X-ray Diffraction* (Dover, New York, 1990).
- ²⁴C. Kittel, *Introduction to Solid State Physics* (Wiley, New York, 1986).
- ²⁵T. Hahn, *International Tables of Crystallography* (Kluwer, Dordrecht, 1987).
- ²⁶E. R. Grilly, *J. Low Temp. Phys.* **11**, 33 (1973).
- ²⁷P. R. Granfors, B. A. Fraass, and R. O. Simmons, *J. Low Temp. Phys.* **67**, 353 (1987).
- ²⁸L. P. Mezhov-Deglin, *Sov. Phys. JETP* **22**, 47 (1966).
- ²⁹C. Kittel, *Quantum Theory of Solids* (Wiley, New York, 1963).
- ³⁰W. R. Gardner, J. K. Hoffer, and N. E. Phillips, *Phys. Rev. A* **7**, 1029 (1973).
- ³¹D. Mills and B. W. Batterman, *Phys. Rev. B* **22**, 2887 (1980).
- ³²N. R. Werthamer, *Solid State Commun.* **9**, 2239 (1971).